Available online at www.sciencedirect.com
SCIENCE DIRECT®
Tetrahedron: Asymmetry
Tetrahedron: *Asymmetry* 16 (2005) 2764–2770

Density functional theory study of the 5-pyrrolidin-2-yltetrazole-catalyzed aldol reaction

Manuel Arnó, Ramón J. Zaragozá and Luis R. Domingo*

Instituto de Ciencia Molecular (UIQOT), Departamento de Química Orgánica, Universidad de Valencia, Dr. Moliner 50, E-46100 Burjassot, Valencia, Spain

Received 16 June 2005; accepted 28 June 2005
Available online 25 July 2005

Abstract—The replacement of the carboxylic acid functionality with a tetrazolic acid in the proline-catalyzed asymmetric aldol reaction between acetone and trimethylacetaldehyde has been studied using DFT methods at the B3LYP/6-31G** computational level. For the C–C bond-formation step, four reactive channels corresponding to the *syn* and *anti* arrangement of the enamine and the *re* and *si* attack modes have been analyzed. The B3LYP/6-31G** results allowed us to explain the stereoselectivity and the increase in reactivity relative to the proline-catalyzed process in DMSO.

1. Introduction

Asymmetric organocatalysis has received much interest in organic chemistry because of the obvious advantages over its metal-mediated counterpart. The advantages are it does not need expensive and often toxic metals, and it is generally easier to make and more easily recoverable than standard catalytic reagents.[1] An organocatalytic molecule that has been studied extensively[2] is proline **1**, which accelerates a range of transformations such as aldol reactions,[3] Robinson annulations[4] and Mannich reactions.[5] Although, these reactions are highly enantioselective, they all rely on fairly polar solvents such as dimethylsulfoxide (DMSO), due to the insoluble nature of proline itself.

The aldol reaction is widely regarded to be one of the most important carbon–carbon bond-formation reaction utilized in organic chemistry.[6] As a result of its utility, extensive efforts have been applied to the development of catalytic enantioselective variants of this reaction. Recently, Hartikka and Arvidsson[7] have studied the 5-pyrrolidin-2-yltetrazole **2** catalyzed aldol reaction of acetone with several aldehydes **3a**–**c** (see Scheme 1). Tetrazoles and carboxylic acids have similar structural requirements and aqueous pK_a values. However, the tetrazole group has increased lipophilicity and metabolic stability.[8] These properties have led to widespread use of tetrazoles in medicinal chemistry as bioisosteres for carboxylic acids. In light of these behaviors, Hartikka and Arvidsson proposed the use of **2** as a more effective catalyst than proline **1**.[7] They found that the increased reactivity of the tetrazole derivative over proline becomes more apparent when less reactive aldehydes are employed as aldol acceptors. In addition, catalyst **2** was shown to be more reactive than proline **1** in several solvents. Regarding the enantioselectivity, no large differences were seen between the two catalysts.

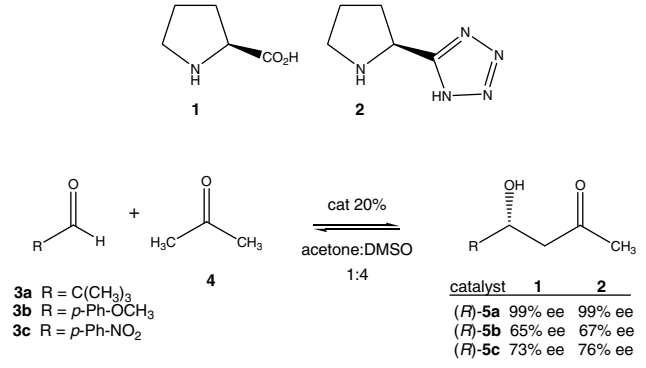

Scheme 1.

Recently, several theoretical studies have been devoted to the proline-catalyzed aldol reaction (see

* Corresponding author. Tel.: +34 96 354 3106; fax: +34 96 354 3152; e-mail: domingo@utopia.uv.es

0957-4166/$ - see front matter © 2005 Elsevier Ltd. All rights reserved.
doi:10.1016/j.tetasy.2005.06.034

Scheme 2).[9,10] These organocatalyzed aldol reactions involve enamine intermediates formed by the condensation of carbonyl compounds with proline. For the C–C bond-formation step, which corresponds with the stereocontrolling step and is presumed to be the rate-determining step for the catalyzed process, four reactive channels corresponding to the *syn* and *anti* arrangement of the active methylene of the enamine relative to the carboxylic acid group of proline, and the two diastereoisomeric approach modes to the *re* and *si* faces of the carbonyl group of the aldehyde were studied.[9] The formation of an intermolecular hydrogen-bond between the acidic hydrogen of proline and the carbonyl oxygen atom of the aldehyde in an early stage of the process catalyzes very effectively the C–C bond formation by a large stabilization of the negative charge which develops at the carbonyl oxygen atom along the nucleophilic attack.[9] The channels associated with the *anti* arrangements of the enamine are favored over the channels associated with the *syn* one, while the attack of the active methylene on the *re* face of the aldehyde is favored over the attack on the *si* face.

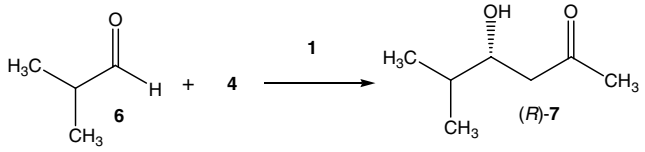

Scheme 2.

Our interest in organocatalysis[9,11] prompted us to carry out a theoretical investigation about the increase of effectiveness by the substitution of the acid functionality of proline by the tetrazolic acid in the aldol reaction using density functional theory (DFT) with the well-established B3LYP/6-31G** method. We have investigated the transitions state structures for the C–C bond-formation step of the tetrazolic acid-catalyzed aldol reaction between trimethylacetaldehyde **3a** and acetone **4** in presence of the 5-pyrrolidin-2-yltetrazole **2** as a model for the catalyzed reactions reported by Hartikka and Arvidsson[7] (see Scheme 1). The transition states associated with the C–C bond-formation step for proline-catalyzed aldol reaction between **3a** and **4** have also been investigated in order to rationalize the increase of catalytic effectiveness with the acid substitution.

2. Computational methods

DFT calculations were carried out using the B3LYP[12] exchange-correlation functional, together with the standard 6-31G** basis set.[13] An exhaustive exploration of the potential energy surfaces (PESs) was carried out to ensure that all relevant stationary points were located and properly characterized. The optimizations were carried out using the Berny analytical gradient optimization method.[14] As minima and transition structures are present as manifold conformers, a minimum conformational search was performed for each structure in order to insure that the selected structure corresponded to the lesser energetic one. The stationary points were characterized by frequency calculations in order to verify that minima and transition structures have zero and one imaginary frequency, respectively. The intrinsic reaction coordinate (IRC)[15] paths were traced in order to check the energy profiles connecting each transition structure to the two associated minima of the proposed mechanism by using the second order González–Schlegel integration method.[16] The electronic structures of stationary points were analyzed by the natural bond orbital (NBO) method.[17] All calculations were carried out with the Gaussian 98 suite of programs.[18]

These aldol reactions were carried out in polar solvents; as the solvent can change both gas phase activation energy and stereoselectivity, their effects were studied. The solvent effects of DMSO, modeled as a continuum model, were considered by B3LYP/6-31G** single point calculations at the gas-phase optimized geometries using a self-consistent reaction field (SCRF)[19] based on the polarizable continuum model (PCM) of Tomasi and co-workers[20] The electronic energies in solution (DMSO) were obtained by adding the total electrostatic energies obtained from the PCM calculations to the electronic energies in vacuo. The PCM and solvent = DMSO options were employed in the SCRF calculations.

3. Results and discussion

The tetrazolic acid can exist mainly as two tautomeric forms in equilibrium (see Scheme 3); the tetrazolic acid form **8** is 2.35 kcal/mol lesser in energy than isomer **9**. With the inclusion of the solvent effect, this difference became 3.34 kcal/mol. Thus, this tautomeric form was assumed for the catalyzed process. For the enamine, two conformational structures are possible due to the restricted rotation around the C4–N5 single bond (see Scheme 4).[9] These conformers relate to the *syn*, **10-s**, and *anti*, **10-a**, arrangement of the active methylene group relative to the tetrazolic acid group. In the gas phase, the conformer **10-s** was 1.26 kcal/mol more stable that **10-a**; however, the easy C4–N5 bond rotation allows an equilibration between these conformers.[9]

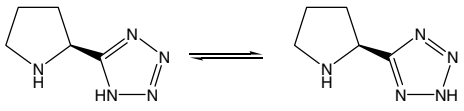

Scheme 3.

The C–C bond-formation step corresponds with the stereocontrol step for the tetrazolic acid-catalyzed aldol reaction. For this step, four reactive channels have been studied. Thus, four transition states, **TS-tar**, **TS-tas**, **TS-tsr**, and **TS-tss**, and their corresponding zwitterionic adducts, **Zw-tar**, **Zw-tas**, **Zw-tsr**, and **Zw-tss**, were localized and characterized (see Scheme 4). These are related to the nucleophilic attack of the active methylene

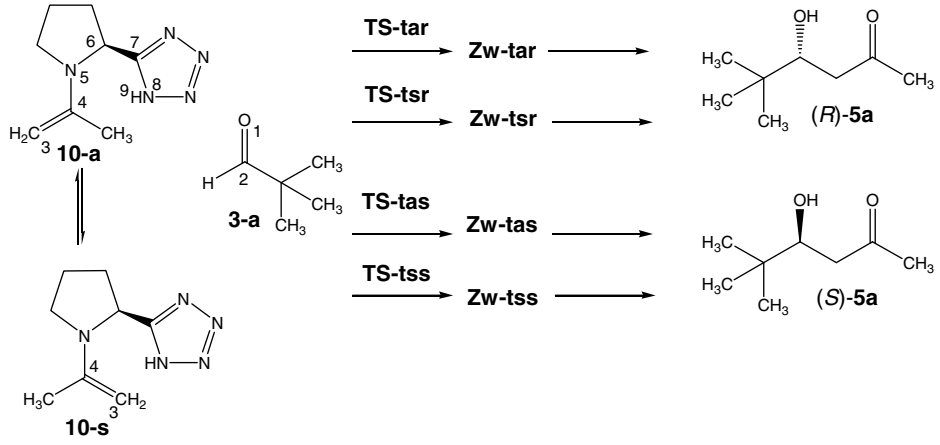

Scheme 4.

of enamines **10-a** and **10-s**, named as **ta** and **ts**, to the *re* and *si* faces of the carbonyl group of tetramethylacetaldehyde **3a**, named as **r** and **s**. The geometries of the transition states and zwitterionic intermediates are shown in Figures 1 and 2, respectively, while the total and relative energies in vacuo and in DMSO are given in Table 1.

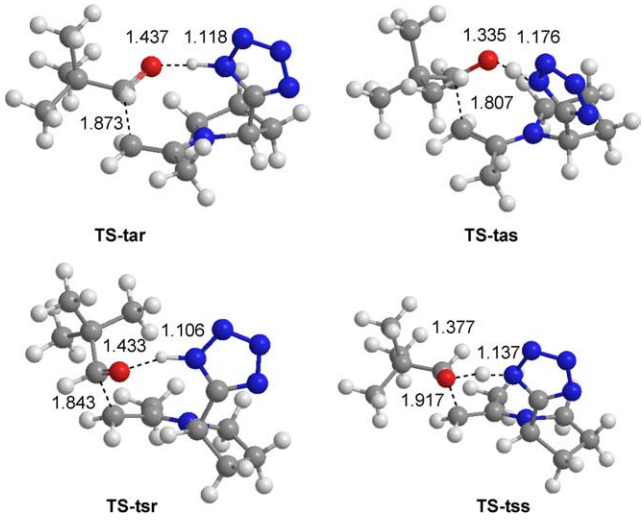

Figure 1. Transition structures corresponding to the C–C bond-formation process for the tetrazolic acid-catalyzed intermolecular aldol reaction between **3a** and **4**. The values of the lengths of the bonds directly involved in the reaction obtained at the B3LYP/6-31G** are given in Angstroms.

The electronic activation energies for the C–C bond formation step relative to the aldehyde **3a** and the *syn* enamine **10-s** are 4.43 (**TS-tar**), 9.49 (**TS-tas**), 13.34 (**TS-tsr**), and 9.41 (**TS-tss**) kcal/mol. The more favorable reactive channel corresponds to the approach of the methylene group of the *anti* enamine **10-a** to the *re* face of the aldehyde **3a** with formation of the zwitterionic intermediate **Zw-tar**, via **TS-tar**. The approach of the methylene group of **10-a** along the *si* face of **3a** with formation of **Zw-tas**, via **TS-tas**, was 5.06 kcal/mol higher in energy than that via **TS-tar**. The zwitterion intermediate **Zw-tar** was located −3.07 kcal/mol below

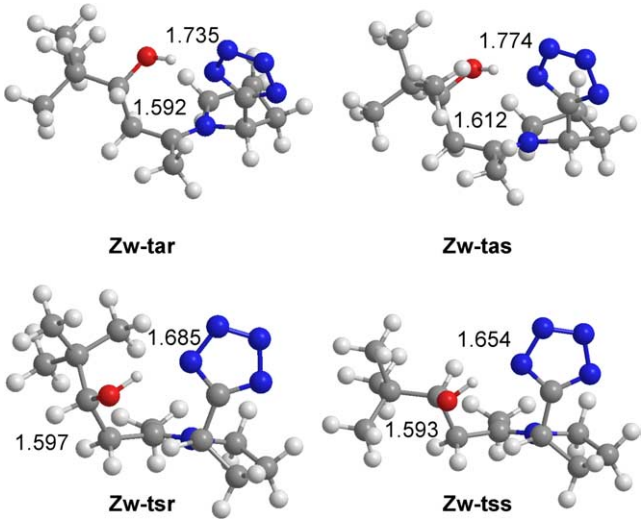

Figure 2. Zwitterionic intermediates for the tetrazolic acid-catalyzed intermolecular aldol reaction between **3a** and **4**. The values of the lengths of the bonds directly involved in the reaction obtained at the B3LYP/6-31G** are given in Angstroms.

10-s + **3a**, while **Zw-tas** was located 2.75 kcal/mol above **10-s** + **3a**. After the formation of the C–C bond, the hydrolysis of the iminium **Zw-tar** was achieved in a series of easy steps that lead to the release of aldol product (*R*)-**5a**.

The inclusion of solvent effects, such as those for DMSO, produces a larger stabilization of the *anti* enamine than the *syn* one. As a consequence, **10-s** is only 0.37 kcal/mol more stable than **10-a**. DMSO stabilizes the transition states between 11 and 13 kcal/mol, while the zwitterionic intermediates are stabilized in ca. 18 kcal/mol. The electronic activation energy for the C–C bond formation along the more favorable reactive channel decreases to 1.99 kcal/mol (**TS-tar**) (see Table 1). The inclusion of solvent effects does not modify substantially the stereoselectivity found in the gas phase. In DMSO, **TS-tas** remains 3.43 kcal/mol more energetic that **TS-tar**. These energetic results are in reasonable agreement with experiments, where ketol (*R*)-**5a** is

Table 1. Total energies (E, au) and relative energies[a] (ΔE, kcal/mol) of the stationary points for the tetrazolic acid-catalyzed and proline-catalyzed intermolecular aldol reaction between **3a** and **4**, in vacuo and in DMSO

	In vacuo		In DMSO	
	E	ΔE	E	ΔE
8	−469.665251		−469.679773	
9	−469.661500	2.35	−469.674447	3.34
3a	−271.787666		−271.790629	
10-s	−586.386844		−586.397747	
10-a	−586.384829	1.26	−586.397164	0.37
TS-tar	−858.167454	4.43	−858.185204	1.99
TS-tas	−858.159383	9.49	−858.179741	5.42
TS-tsr	−858.153252	13.34	−858.171355	10.68
TS-tss	−858.159517	9.41	−858.177873	6.59
Zw-tar	−858.179397	−3.07	−858.207922	−12.27
Zw-tas	−858.170132	2.75	−858.198503	−6.36
Zw-tsr	−858.165381	5.73	−858.194198	−3.65
Zw-tss	−858.172820	1.06	−858.200450	−7.58
11-s	−517.889316		−517.897328	
TS-par	−789.670564	4.03	−789.682330	3.53
TS-pas	−789.663975	8.16	−789.675478	7.83
Zw-par	−789.690542	−8.51	−789.707882	−12.50
Zw-pas	−789.682556	−3.50	−789.700094	−7.62

[a] Relative to **3a** and **10-s** or **3a** and **11-s**.

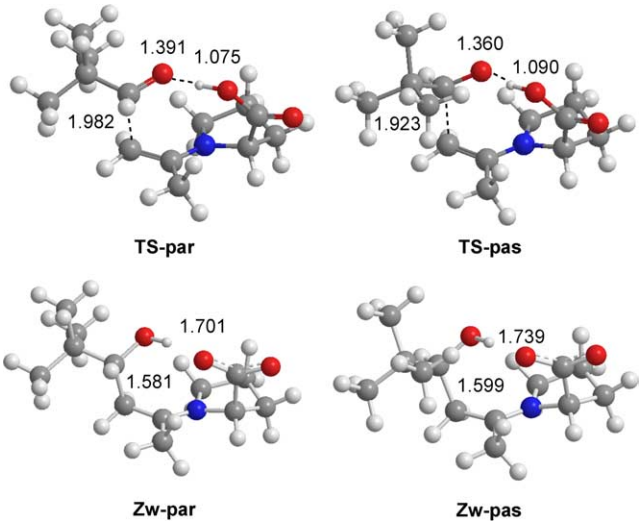

Figure 3. Transition structures and zwitterionic intermediates corresponding to the C–C bond-formation process for the proline-catalyzed intermolecular aldol reaction between **3a** and **4**. The values of the lengths of the bonds directly involved in the reaction obtained at the B3LYP/6-31G** are given in Angstroms.

isolated in 99% of enantiomeric excess (ee) (see Scheme 1).[7] Note that the predicted stereoselectivity is about an order of magnitude higher than the experimental; both predicted and experimental ee are high, and are in the same direction.

In order to rationalize the role of the tetrazolic acid substitution on the organocatalyst process, the *anti* channels associated with the C–C bond formation step for the proline-catalyzed aldol reaction between **3a** and **4** were also studied (see Scheme 5). Thus, two transition states, **TS-par** and **TS-pas**, and two zwitterionic intermediates, **Zw-par** and **Zw-pas**, associated with the approach of the methylene group in the *anti* conformation of the enamine, **11-a**, along the *re* and *si* faces of aldehyde **3a**, were localized and characterized. The geometries of the transition states and the zwitterionic intermediates are shown in Figure 3, while the total and relative energies in vacuo and in DMSO are given in Table 1. The electronic activation energy for the C–C bond-formation step was 4.03 (**TS-par**) and 8.16 (**TS-pas**) kcal/mol. **TS-pas** was 4.13 kcal/mol higher in energy than **TS-par**, which is in clear agreement with the large enantioselectivity observed experimentally (99% ee).[7] Inclusion of solvent effects reduces the electronic activation energies of **TS-par** and **TS-pas**, 1.50 and 0.33 kcal/mol, respectively. In DMSO, the stereoselectivity found in the gas phase was not modified.

The more noticeable effect with the inclusion of solvent effects is that in DMSO, the activation energy for the tetrazolic acid-catalyzed process is lower than that for the proline-catalyzed one, in agreement with the experimental outcome. These results are a consequence of a larger solvation of **TS-tar** (11.14 kcal/mol) than **TS-par** (7.38 kcal/mol). In both tetrazolic acid and proline-catalyzed processes, the intramolecular hydrogen-bond between the acidic hydrogen and the carbonyl oxygen atom is responsible for the large catalytic effect observed at these organocatalyzed aldol reactions.[9] The more acidic character of the NH group in tetrazole in comparison with the COOH one in proline, favors a larger charge transfer at **TS-tar** than at **TS-par**, while a larger acceleration was found for the tetrazolic acid-catalyzed process in DMSO as a consequence of a larger solvation of the former transition state.

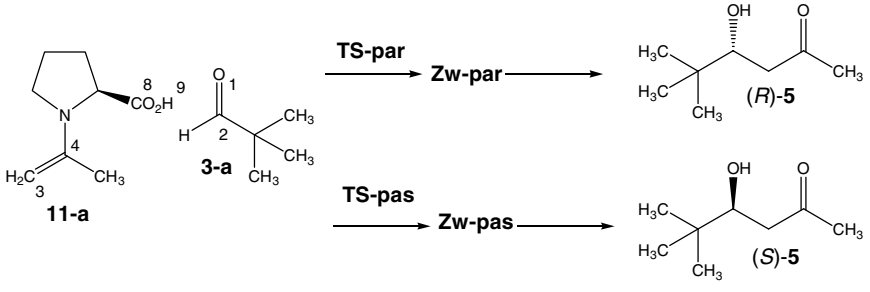

Scheme 5.

Along the C–C bond-formation pathway for the tetrazolic acid-catalyzed process, the lengths of the C2–C3 forming bond at **TS-tar**, **TS-tas**, **TS-tsr** and **TS-tss**, were 1.873, 1.807, 1.843, and 1.917 Å, respectively. The O1–H9 and N8–H9 lengths at these transition states are 1.437 and 1.118 Å in **TS-tar**, 1.335 and 1.176 Å in **TS-tas**, 1.433 and 1.106 Å in **TS-tsr**, and 1.377 and 1.137 Å in **TS-tss**. At the zwitterionic intermediates, the lengths of the C2–C3 bond are in the range 1.59–1.61 Å, while the distance between the hydroxyl H9 hydrogen and the tetrazole N8 nitrogen are in the range 1.65–1.77 Å. These distances point out an intramolecular hydrogen-bond between the hydroxyl H9 hydrogen and the tetrazole N8 nitrogen (see Fig. 2). It is noteworthy that tetrazole supports the negative charge at these zwitterionic intermediates.

In the proline-catalyzed process, the lengths of the C2–C3 forming bond at **TS-par** and **TS-pas** were 1.982 and 1.923 Å, respectively, while the O1–H9 and O8–H9 lengths were 1.391 and 1.075 Å at **TS-par**, and 1.360 and 1.090 Å at **TS-pas**, respectively. The C–C lengths at the tetrazolic acid-catalyzed process are slightly shorter than those associated with the proline-catalyzed one. In the zwitterionic intermediates, the C2–C3 bond length was 1.581 Å in **Zw-par** and 1.599 Å in **Zw-pas**. The distance between the hydroxyl H9 hydrogen and the carboxylate O8 oxygen was 1.701 in **Zw-par** and 1.739 Å in **Zw-pas**. These distances show an intramolecular hydrogen bond between the hydroxyl H9 hydrogen and the carboxylate O8 oxygen of the proline residue.

A conformational analysis at the more favorable *anti* transition states shows that while at **TS-tar**, the C2–C3 forming bond presents a *gauche* arrangement between the carbonyl oxygen atom and the enamine framework, the O1–C2–C3–C4 dihedral angle is 54.5°, the less favorable **TS-tas** presents two *gauche* arrangements between the enamine framework and the carboxyl oxygen atom and the *tert*-butyl group of the aldehyde **3a**; the O1–C2–C3–C4 and C10–C2–C3–C4 dihedral angles are 36.2° and −97.6°, respectively (see Fig. 4). Therefore, the steric hindrance which appears between the *tert*-butyl group belonging to aldehyde **3a** and the methyl group of enamine **10-a** at **TS-tas** is responsible for the larger energy of the latter relative to **TS-tar**, and as a result the enantioselectivity showed at this tetrazolic acid-catalyzed aldol reaction.

The values of the unique imaginary frequency associated with **TS-tar**, **TS-tas** **TS-tsr**, and **TS-tss** are 269i, 357i, 533i, and 269i cm^{-1}, respectively. Analysis of the atomic movement associated with these imaginary frequency indicates that these transition states are associated mainly with the movement of the C2 and C3 carbon atoms along the C2–C3 bond formation, and the coupled movement of the acidic H9 hydrogen atom along the proton transfer process. Therefore, the C2–C3 bond formation and the proton transfer are coupled processes at these transition states.

The Wiberg bond order[21] (BO) values of the C2–C3 forming bond at **TS-tar**, **TS-tas**, **TS-tsr**, and **TS-tss** are

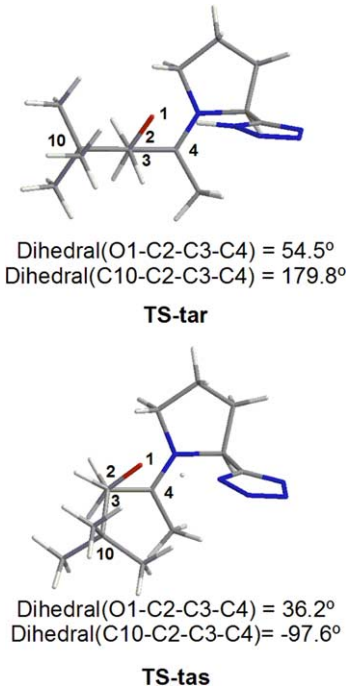

Figure 4. *Anti* and *gauche* arrangement of the *tert*-butyl group, C10–C2–C3–C4 dihedral angles, along the C–C bond formation at the more favorable *anti* transition states.

0.59, 0.69, 0.64, and 0.57, respectively. The BO values of the O1–H9 and N8–H9 bonds at these transition states are 0.21 and 0.54 at **TS-tar**, 0.27 and 0.47 at **TS-tas**, 0.20 and 0.54 at **TS-tsr**, and 0.23 and 0.51 at **TS-tss**, respectively. Therefore, the proton transfer process is slightly more delayed than the C–C bond formation one.[9] Finally, the BO value of the C4–N5 bond at these transition states, ca. 1.4, indicate a large π character for the C4–N5 single bond as a consequence of the large participation of N5 lone pair on the C–C bond-formation process.[9] In the transition states associated with the proline-catalyzed process, the BO values of the C2–C3 forming bond are 0.51 in **TS-par** and 0.58 in **TS-pas**. The BO values of the O1–H9 and O8–H9 bonds at these transition states are 0.23 and 0.48 at **TS-par**, 0.25 and 0.45 at **TS-pas**. A comparison of the BO values at **TS-tar** and **TS-par** indicated that the C–C bond formation and the proton transfer processes at the tetrazolic acid-catalyzed process are slightly more advanced than those at the proline catalyzed process.

Finally, the natural population analysis (NPA)[17a] allows us to evaluate the charge transfer along the C–C bond-formation process. Analysis of the natural charges at the atoms belonging to the carbonyl groups O1 and C2 allows us to evaluate the charge transfer in the transition states along the nucleophilic attack of the enamines **10-s**, **10-a** and **11-a** to the aldehyde **3a** (see Table 2). The charge transferred to the carbonyl group at the transition states are 0.45 e at **TS-tar**, 0.49 e at **TS-tas**, 0.44 e at **TS-tsr** and 0.39 e at **TS-tss**. 0.37 e at **TS-par** and 0.43 e at **TS-pas**. For the tetrazolic acid-catalyzed process, there are larger charge transfers at the more favorable *anti* transition states than at the *syn* ones. In

Table 2. Natural charges and charge transfer (in au) to the carbonyl group at the tetrazolic acid-catalyzed and proline-catalyzed aldol reaction between **3a** and **4**

	TS-tar	TS-tas	TS-tsr	TS-tss	TS-par	TS-pas
	Natural charges					
O1	−0.79	−0.81	−0.78	−0.75	−0.74	−0.78
C2	0.24	0.22	0.25	0.26	0.27	0.25
C3	−0.74	−0.59	−0.61	−0.61	−0.60	−0.60
C4	0.38	0.41	0.37	0.36	0.35	0.37
N5	−0.37	−0.36	−0.36	−0.37	−0.38	−0.37
	Charges on groups					
C=O	−0.54	−0.59	−0.54	−0.49	−0.47	−0.53
N–C=C	−0.73	−0.54	−0.60	−0.62	−0.63	−0.60
	Charge transfer to the carbonyl group					
	−0.45	−0.49	−0.44	−0.39	−0.37	−0.43

addition, for the tetrazolic acid-catalyzed process, the charge transfer at the more favorable channel, −0.45 e (**TS-tar**), is larger than that at the proline-catalyzed process, −0.37 e (**TS-par**). This analysis is in agreement with the larger dipole moment of **TS-tar**, 8.94 Debye, than **TS-par**, 6.60 Debye, and as a consequence, with the larger solvation of the former. As a result, the large acidic character of tetrazole, which permits a more advanced C–C bond-formation process than that for the proline catalyzed process, allows us to explain the larger effectiveness of the tetrazolic acid group than the carboxylate one in the proline as catalyst in DMSO.[7] Finally, an analysis of the natural charges at the zwitterionic intermediates formed along the C–C bond formation indicates that the negative charge in these zwitterionic species is located mainly on the tetrazole and the carboxylate as a consequence of the proton transfer to the alcoxide O1 oxygen along these acid catalyzed processes.

4. Conclusions

The transition structures associated with the C–C bond-formation step of the tetrazolic acid-catalyzed aldol reaction between acetone and trimethylacetaldehyde have been studied using DFT methods at the B3LYP/6-31G** computational level. For this stereocontrolling step, four reactive channels corresponding to the *syn* and *anti* arrangement of the active methylene of the enamine relative to the tetrazole group, and the two diastereoisomeric approach modes to the *re* and *si* faces of the carbonyl group of the aldehyde have been studied. The formation of an intermolecular hydrogen bond between the acidic hydrogen of tetrazole and the carbonyl oxygen atom of the aldehyde catalyzes very effectively the C–C bond formation by a large stabilization of the negative charge that develops at the carbonyl oxygen atom along with the nucleophilic attack. As a consequence of the hydrogen-bond formation, the reactive channels associated with the *anti* arrangement of the methylene of the enamine are favored over the channels associated with the *syn* arrangement. In addition, along with the *anti* channels the attack of the active methylene on the *re* face of the aldehyde is favored over the attack on the *si* face in agreement with the experiments.

Conformational analysis along the C–C forming bond in the transition states associated with the *anti* channels shows that the *gauche* interaction between the *tert*-butyl group of the aldehyde and the methyl group of the enamine present at **TS-tas** is responsible for the large diastereoselectivity observed experimentally. Finally, the larger charge transfer found in the transition states associated with the tetrazolic acid-catalyzed process than those associated with the proline-catalyzed one, allows us to explain the larger catalytic efficiency of the tetrazolic acid group by a larger solvation of the transition state involved in the tetrazolic acid-catalyzed process. This DFT study is in reasonable agreement with the available experiments, allowing us to explain the large effectiveness of the tetrazole group in the catalyzed aldol reactions of acetone with the aldehydes reported recently by Hartikka and Arvidsson.[7]

Acknowledgements

This work was supported by research funds provided by the Ministerio de Ciencia y Tecnología of the Spanish Government by DGICYT (project BQU2002-01032) and by the AVCYT of the Generalitat Valenciana (reference GRUPOS03/176).

References

1. Dalko, P. I.; Moisan, L. *Angew. Chem., Int. Ed.* **2001**, *40*, 3726.
2. List, B. *Tetrahedron* **2002**, *58*, 5573.
3. (a) Hajos, Z. G.; Parrish, D. R. *J. Org. Chem.* **1974**, *39*, 1615; (b) List, B.; Pojarliev, P.; Castello, C. *Org. Lett.* **2001**, *3*, 537; (c) Szollosi, G.; Lonfon, G.; Balaspiri, L.; Somlai, C.; Bartok, M. *Chirality* **2003**, *15*, S90; (d) Northrup, A. B.; MacMillan, D. W. C. *J. Am. Chem. Soc.* **2002**, *124*, 6798.
4. (a) Bui, T.; Barbas, C. F., III. *Tetrahedron Lett.* **2000**, *41*, 6951; (b) Rajagopal, D.; Narayanan, R.; Swaminathan, S. *Tetrahedron Lett.* **2001**, *42*, 4887.
5. (a) Córdova, A.; Notz, W.; Zhong, G.; Betancort, J. M.; Barbas, C. F., III. *J. Am. Chem. Soc.* **2002**, *124*, 1842; (b) Córdova, A.; Watanabe, S.-i.; Tanaka, F.; Notz, W.; Barbas, C. F., III. *J. Am. Chem. Soc.* **2002**, *124*, 1866; (c) Pojarliev, P.; Biller, W. T.; Martin, H. J.; List, B. *Synlett*

2003, 1903; (d) Chowdari, N. S.; Ramachary, D. B.; Barbas, C. F., III. *Synlett* **2003**, 1906; (e) Notz, W.; Tanaka, F.; Watanabe, S.-i.; Chowdari, N. S.; Turner, J. M.; Thayumanavan, R.; Barbas, C. F., III. *J. Org. Chem.* **2003**, *68*, 9624; (f) Itoh, T.; Yokoya, M.; Miyauchi, K.; Nagata, K.; Ohsawa, A. *Org. Lett.* **2003**, *5*, 4301.

6. (a) Masamune, S.; Choy, W.; Peterson, J.; Sita, L. R. *Angew. Chem., Int. Ed. Engl.* **1985**, 1; (b) Evans, D. A. *Science* **1988**, *240*, 420; (c) Heathcock, C. H. *Aldrichim. Acta* **1990**, *23*, 99; (d) Cowden, C. J.; Paterson, I. *Org. React.* **1997**, *51*, 1; (e) Franklin, A. S.; Paterson, I. *Contemp. Org. Synth.* **1994**, *1*, 317.
7. Hartikka, A.; Arvidsson, P. I. *Tetrahedron: Asymmetry* **2004**, *15*, 1831.
8. (a) Butler, R. N. In *Comprehensive Heterocyclic Chemistry*; Katritzky, A. R., Rees, C. W., Scriven, E. F. V., Eds.; Pergamon: Oxford, UK, 1996; Vol. 4; (b) Herr, R. *J. Bioorg. Med. Chem.* **2002**, *10*, 3379.
9. Arnó, M.; Domingo, L. R. *Theor. Chem. Acc.* **2002**, *108*, 232.
10. (a) Rankin, K. N.; Gauld, J. W.; Boyd, R. J. *J. Phys. Chem. A* **2002**, *106*, 5155; (b) Bahmanyar, S.; Houk, K. N.; Martin, H. J.; List, B. *J. Am. Chem. Soc.* **2003**, *125*, 2475; (c) Clemente, F. R.; Houk, K. H. *Angew. Chem., Int. Ed.* **2004**, *43*, 5766.
11. (a) Arnó, M.; Domingo, L. R. *Org. Biomol. Chem.* **2003**, *1*, 637; (b) Arnó, M.; Zaragozá, R. J.; Domingo, L. R. *Tetrahedron: Asymmetry* **2004**, *15*, 1541.
12. (a) Becke, A. D. *J. Chem. Phys.* **1993**, *98*, 5648; (b) Lee, C.; Yang, W.; Parr, R. G. *Phys. Rev. B* **1988**, *37*, 785.
13. Hehre, W. J.; Radom, L.; Schleyer, P. v. R.; Pople, J. A. *Ab initio Molecular Orbital Theory*; Wiley: New York, 1986.
14. (a) Schlegel, H. B. *J. Comput. Chem.* **1982**, *3*, 214; (b) Schlegel, H. B. Geometry Optimization on Potential Energy Surface. In *Modern Electronic Structure Theory*; Yarkony, D. R., Ed.; World Scientific Publishing: Singapore, 1994.
15. Fukui, K. *J. Phys. Chem.* **1970**, *74*, 4161.
16. (a) González, C.; Schlegel, H. B. *J. Phys. Chem.* **1990**, *94*, 5523; (b) González, C.; Schlegel, H. B. *J. Chem. Phys.* **1991**, *95*, 5853.
17. (a) Reed, A. E.; Weinstock, R. B.; Weinhold, F. *J. Chem. Phys.* **1985**, *83*, 735; (b) Reed, A. E.; Curtiss, L. A.; Weinhold, F. *Chem. Rev.* **1988**, *88*, 899.
18. Frisch, M. J.; Trucks, G. W.; Schlegel, H. B.; Scuseria, G. E.; Robb, M. A.; Cheeseman, J. R.; Zakrzewski, V. G.; Montgomery, J. A., Jr.; Stratmann, R. E.; Burant, J. C.; Dapprich, S.; Millam, J. M.; Daniels, A. D.; Kudin, K. N.; Strain, M. C.; Farkas, O.; Tomasi, J.; Barone, V.; Cossi, M.; Cammi, R.; Mennucci, B.; Pomelli, C.; Adamo, C.; Clifford, S.; Ochterski, J.; Petersson, G. A.; Ayala, P. Y.; Cui, Q.; Morokuma, K.; Malick, D. K.; Rabuck, A. D.; Raghavachari, K.; Foresman, J. B.; Cioslowski, J.; Ortiz, J. V.; Stefanov, B. B.; Liu, G.; Liashenko, A.; Piskorz, P.; Komaromi, I.; Gomperts, R.; Martin, R. L.; Fox, D. J.; Keith, T.; Al-Laham, M. A.; Peng, C. Y.; Nanayakkara, A.; Challacombe, M.; Gill, P. M. W.; Johnson, B.; Chen, W.; Wong, M. W.; Andres, J. L.; Gonzalez, C.; Head-Gordon, M.; Replogle, E. S.; Pople, J. A. Gaussian 98, Revision A.6 Gaussian, Inc.: Pittsburgh PA, 1998.
19. (a) Tomasi, J.; Persico, M. *Chem. Rev.* **1994**, *94*, 2027; (b) Simkin, B. Y.; Sheikhet, I. *Quantum Chemical and Statistical Theory of Solutions—A Computational Approach*; Ellis Horwood: London, 1995.
20. (a) Cossi, M.; Barone, V.; Cammi, R.; Tomasi, J. *Chem. Phys. Lett.* **1996**, *255*, 327; (b) Cances, E.; Mennucci, B.; Tomasi, J. *J. Chem. Phys.* **1997**, *107*, 3032; (c) Barone, V.; Cossi, M.; Tomasi, J. *J. Comput. Chem.* **1998**, *19*, 404.
21. Wiberg, K. B. *Tetrahedron* **1968**, *24*, 1083.